DIABETES/METABOLISM RESEARCH AND REVIEWS
Diabetes Metab Res Rev 2010; **26**: 40–49.
Published online 10 December 2009 in Wiley InterScience (www.interscience.wiley.com) **DOI:** 10.1002/dmrr.1054

RESEARCH ARTICLE

miR133a regulates cardiomyocyte hypertrophy in diabetes

Biao Feng[1]
Shali Chen[1]
Biju George[1]
Qingping Feng[2]
Subrata Chakrabarti[1]*

[1]*Department of Pathology, Schulich School of Medicine & Dentistry, University of Western Ontario, London, Ontario, Canada*

[2]*Department of Physiology and Pharmacology, Schulich School of Medicine & Dentistry, University of Western Ontario, London, Ontario, Canada*

*Correspondence to:
Subrata Chakrabarti, Department of Pathology, Schulich School of Medicine & Dentistry, University of Western Ontario, DSB-4030, London, Ontario N6A 5C1, Canada.
E-mail: subrata.chakrabarti@schulich.uwo.ca

Received: 1 September 2009
Revised: 14 October 2009
Accepted: 20 October 2009

Abstract

Background Diabetic cardiomyopathy, characterized by cardiac hypertrophy and contractile dysfunction, eventually leads to heart failure. We have previously shown that alterations of a number of key molecules are involved in producing cardiomyocyte hypertrophy in diabetes. The aim of the present study was to determine whether microRNAs (miRNA) play a role in mediating altered gene expression and structural/functional deficits in the heart in diabetes.

Methods STZ-induced diabetic mice were haemodynamically investigated after 2 months of diabetes to establish the development of cardiomyopathy. The tissues were then examined for gene expression and microRNA analysis. We further investigated neonatal rat cardiomyocytes to identify the mechanisms of glucose-induced hypertrophy and the potential role of miR133a.

Results Diabetic mice showed myocardial contractile dysfunction and augmented mRNA expression of atrial and brain natriuretic peptides (ANP, BNP), MEF2A and MEF2C, SGK1 and IGF1R compared to age- and sex-matched controls. Cardiac tissues from these mice showed alteration of multiple miRNAs by array analysis including miR133a, which was confirmed by RT-PCR. *In vitro* exposure of cardiomyocytes to high levels of glucose produced hypertrophic changes and reduced expression of miRNA133a. Finally, transfection of miR133a mimics prevented altered gene expression and hypertrophic changes.

Conclusion Data from these studies demonstrate a novel glucose-induced mechanism regulating gene expression and cardiomyocyte hypertrophy in diabetes which is mediated through miR133a. Copyright © 2009 John Wiley & Sons, Ltd.

Keywords diabetes; cardiomyocytes; hypertrophy; miRNA

Abbreviations α-MHC – α-myosin heavy chain; ANP – atrial natruiretic peptide; BCA – bicinchoninic acid; BNP – brain natruiretic peptide; HAT – histone acetyltransferase; HDAC – histone deacetylase; IGF1R – insulin-like growth factor-1 receptor; LVEDP – left ventricle end-diastolic pressure; MEF2 – myocyte enhancer factor-2; MEM – minimum essential medium; NF-κB – nuclear factor-kappa B; STZ – streptozotocin; SGK1 – serum- and glucocorticoid-regulated kinase 1

Introduction

Cardiomyocyte hypertrophy leading to cardiac failure is one of the characteristic alterations in diabetic cardiomyopathy [1]. Several regulatory

mechanisms are involved in mediating alteration of gene transcription, effector protein production and subsequent structural changes in such process. Alteration of protein production may also occur at the translational levels through microRNAs (miRNAs) [2].

miRNAs are small (~20–25 nucleotide) RNA molecules that have significant effects on the regulation of gene expression [3]. The transcription of the miRNA occurs through RNA polymerase II and subsequent processing to precursor miRNAs (70–100 nucleotides, hairpin-shaped) in the nucleus is mediated by RNAse III Dorsha and DGCR8. Following synthesis, miRNAs are exported to the cytoplasm by exportin 5. A fully active form is formed in the cytoplasm following further processing by Dicer [3,4]. miRNAs bind to the specific mRNA targets causing their degradation or translational repression [3,4]. Several investigators, using overexpression experiments, have demonstrated importance of miRNAs in diverse cellular processes [3,5]. It has been postulated that epigenetic mechanisms play a fundamental role in the regulation of miRNAs [3].

In the context of heart failure, alterations in several miRNAs have been demonstrated in the mouse heart following aortic banding or similar insult [6,7]. These studies have also reported that in neonatal cardiomyocytes miR21 and miR195 mediates signalling in phenylephrine or angiotensin II induced hypertrophy [6,7]. In neonatal cardiomyocytes, experiments have also demonstrated that α-MHC regulates cardiac growth and gene expression in response to stress and hormonal signalling through miR208, which is encoded by α-MHC intron [8]. miR133a has also been shown to regulate cardiomyocyte proliferation and suppress smooth muscle gene expression in the heart [9]. It has also been demonstrated that MEF2 dependent enhancer directs expression of miR133 [10]. Recently, one study has examined hearts from diabetic rabbit and that demonstrated increase in miR133, modulating HERG K+ channel and causing QT prolongation [11]. Although miR133 has been shown to be decreased during skeletal muscle hypertrophy [12], contrasting findings have been obtained with respect to the role of miR133 in hypertrophic cardiomyopathy [13–16]. Moreover, no studies have yet specifically examined miRNAs in the context of cardiomyocyte hypertrophy in diabetes. Therefore, the aim of the present study was to determine whether diabetes leads to aberrant expression of miRNAs including miR133a. In order to determine the functional significance of miRNA alteration, we also used an *in vitro* model of hyperglycemia-induced cardiomyocyte hypertrophy.

Materials and methods

Animal experiments

The animal experiments were performed in accordance with regulations specified by the Canadian Council on Animal Care. The University of Western Ontario Animal Care and Veterinary services approved all experiments. In addition, this investigation conforms to the Guide for the Care and Use of Laboratory Animals published by the US National Institutes of Health (NIH Publication No. 85-23, revised 1996).

C57BL/6J mice were obtained from Jackson laboratories (Bar harbour, Maine, USA). Beginning at 6 weeks of age, the mice were randomly divided in two groups. One group of male mice were made diabetic by intraperitoneal injection of STZ [three 50 mg/kg consecutive injection on alternate days in citrate buffer, pH = 5.6]. Sex-matched littermates were used as controls and were given an equal volume of citrate buffer. Diabetes was defined as blood glucose level >20 mmol/L on two consecutive days (Freestyle Mini, TheraSense Inc., Alameda, CA, USA). The animals were fed on a standard rodent diet and water *ad libitum* and were monitored for hyperglycemia, glucosuria and ketonuria (Uriscan Gluketo™, Yeong Dong Co., Seoul, South Korea) [17–20]. None of the animals received exogenous insulin. The animals ($n = 6$ per group) were sacrificed after 2 months of diabetes. Haemodynamic assessment was carried out just before sacrifice and cardiac tissues were harvested at the time of sacrifice and snap-frozen.

Haemodynamic assessment

Mice were anesthetized with intraperitoneal injections of ketamine (50 mg/kg) and xylazine (10 mg/kg). Measurements of LV pressure were obtained using a pressure-conductance catheter (SPR-839, 1.4F, Millar Instruments, TX, USA) as previously described [21]. Briefly, the catheter was calibrated at the beginning of each experiment and inserted into the right carotid artery for recording the arterial pressure under a dissecting microscope. The catheter was then advanced retrograde into the LV for recording of LV pressures, volumes, and heart rate. Signals were fed to an analog digital converter and collected by a PowerLab Chart program (ADInstruments, Colorado Springs, CO). All haemodynamic parameters including LV systolic pressure, LVEDP, ejection fraction and maximal positive and minimal negative revised derivative of LV pressure ($+dP/dt$ max and $-dP/dt$ min) were analysed by a PVAN software (Millar Instruments, Houston, TX).

Isolation and culture of neonatal cardiomyocytes

Neonatal rat myocytes were isolated from new-born Harlan Sprague-Dawley rat heart ventricles as described previously [10]. Non-myocytes were removed by differential attachment as described. Furthermore, the cells were characterized by light microscopy and immunostaining [22,23]. Isolated cardiomyocytes were plated onto 6 cm cell culture dishes (Primaria™ Tissue Culture Dish, Becton Dickinson, USA) at a density of 3.0×10^4 cells/cm^2 and were maintained for 48 h in Dulbecco's

DOI: 10.1002/dmrr

Modified Eagle's Medium/Ham's F-12 supplemented with 10% fetal bovine serum, 10 μg/mL transferrin, 10 μg/mL insulin, 10 ng/mL selenium, 50 units/mL penicillin, 50 μg/mL streptomycin, 2 mg/mL bovine serum albumin, 5 μg/mL linoleic acid, 3 mmol/L pyruvic acid, 0.1 mmol/L MEM non-essential amino acids, 10% MEM vitamin, 0.1 mmol/L bromodeoxyuridine, 100 μM L-ascorbic acid, and 30 mmol/L HEPES (pH 7.1). The cells were serum-starved overnight prior to all experiments. Unless otherwise stated, all chemicals were of reagent-grade quality and were purchased from Sigma Chemical (Sigma, Oakville, ON, Canada). All experiments were carried out after 48 h of incubation with 5 mmol/L (control) or 25 mmol/L glucose (high glucose; HG), unless otherwise indicated. Twenty-five mmol/L L-glucose was used as osmotic control. All experiments were repeated with at least two different cardiomyocyte preparations and in triplicates.

Microarray analysis for miRNA expression

MicroRNAs were extracted from cardiac tissues using the mirVana miRNA isolation kit (Ambion Inc., Austin, TX, USA). Briefly, the tissues were homogenized in the Lysis/Binding solution. miRNA additive (1 : 10) and equal volume acid-phenol : chloroform was added to the lysate and incubated for 10 min on ice. Following centrifugation and removal of the aqueous phase, the mixture was incubated in ethanol. The mixture was passed through the filter cartridge and was eluted with elution solution.

miRNA expression profiling was performed as described by others [7]. In brief, 10 μg of isolated RNA was labeled with Cy5 mono-functional NHS ester (GE Healthcare, UK) and hybridized with a mirVana miRNA Bioarrays (Ambion Inc., Austin, TX, USA). These arrays comprise of a mixture of oligoribonucleotide probes for 486 mature miRNAs in SLF-0601 disposable chambers (MJ Research, Bio-Rad, USA). Arrays were scanned using a BioRad VersArray ChipReader (BioRad, Mississauga, ON) at 5 μm resolution. The resultant image files were analysed using Array Vision 6.0 (GE Healthcare, Fairfield, CT). Background subtracted data was imported into GeneSpring GX 7.3.1 (Agilent Technologies Inc., Palo Alto, CA). Data were then transformed (measurements less than 1.0 set to 1.0), normalized per chip to the 50th percentile of the control_1 spots and per gene to each normal sample for each slide. Using a twofold cut-off, genes that were either increased or decreased at least twofold in each array were then selected. Normalized data were hierarchically clustered by gene and plotted as a heat map.

miRNA analysis by RT-PCR

miRNAs were isolated using mirVana kit (Ambion Inc., Austin, TX, USA). Real-time PCR was used to validate array data. The primers were obtained from Ambion Inc. (Austin, TX, USA). For a final reaction volume of 20 μL, the following reagents were added: 10 μL TaqMan 2× Universal PCR Master Mix (No AmpErase UNG), 8 μL Nuclease-free water, 1 μL TaqMan microRNA probe and 1 μL cDNA product. The data was normalized to RNU6B to account for differences in reverse-transcription efficiencies and amount of template in the reaction mixtures.

Western blotting

Rat myocytes were centrifuged and resuspended in ice-cold RIPA lysis buffer (0.5 M Tris–HCl, pH 7.4, 1.5 M NaCl, 2.5% deoxycholic acid, 10% NP-40, 10 mM EDTA). Cell lysates were subsequently sonicated and the protein was quantified by BCA assay (Pierce Endogen, IL, USA). To confirm expression of MEF2, SGK1 and IGF1R, 30 μg of protein was loaded and size-fractionated on a 10% SDS–PAGE and blotted overnight onto a PVDF membrane (BIO-RAD Hercules, CA, USA). Nonspecific sites were blocked in a 5% solution of nonfat milk powder in TBS. The PVDF membrane was incubated with high-affinity rabbit polyclonal anti-MEF2 (recognizes both MEF2A and MEF2C), SGK1, p-SGK1 and IGF1R antibodies (Santa Cruz Biotechnology Inc., CA, USA) followed by incubation with goat anti-rabbit secondary IgG antibody with horseradish peroxidase conjugate (Santa Cruz Biotechnology Inc., CA, USA) using 1 : 1000 and 1 : 5000 dilutions, respectively. Lysates containing MEF2 were visualized with enhanced chemiluminescence Advance Western blot detection system (Amersham Biosciences, Piscataway, NJ, USA) and Alphaimager 2200. β-actin expression was tested using the same membrane as an internal control.

miRNA mimic transfection

The cardiomyocytes were transfected with miRIDIAN micro RNA Mimic miR133a (20 nM) (DHARMACON Inc., Chicago, IL, USA) using transfection reagent (Qiagen, ON, Canada). The constructs were custom synthesized from Dharmacon Inc. Related oligonucleotide sequences, based on *Caenorhabditis elegans* miRNA with similar design and modifications as miRIDIAN microRNA mimics, were used negative control miRNA (20 nM) for control transfection. miRNA transfection efficiency was determined by real-time RT-PCR.

Cell viability

Cell viability was examined by trypan blue dye exclusion test. Trypan blue stain was prepared fresh as a 0.4% solution in 0.9% sodium chloride. The cells were washed in PBS, trypsinized, and centrifuged. Twenty microlitres of cell suspension were added to 20 μL of trypan blue solution and 500 cells were microscopically counted

DOI: 10.1002/dmrr

in Burker cytometer. Cell viability was expressed as a percentage of the trypan blue negative cells in untreated controls [22,23].

Morphometric analysis

Cardiomyocyte cell surface area was measured to assess cellular hypertrophy using previously described methodology [22]. Cells were visualized with a Leica inverted microscope and images were captured at 20× magnification. Cell area was determined using Mocha™ Software (SPSS, IL, USA). Cardiomyocyte surface area was determined from 100 randomly selected cells per culture plate and expressed as μm^2.

RNA extraction and RT-PCR

RNA was extracted with TRIzol™ reagent (Invitrogen Canada Inc., ON, Canada) as previously described [22,24]. Total RNA (2 μg) was used for cDNA synthesis with oligo (dT) primers (Invitrogen Canada Inc., ON, Canada). Reverse transcription was carried out by the addition of Superscript™ reverse transcriptase (Invitrogen Canada Inc., ON, Canada). The resulting cDNA products were stored at −20 °C. Real-time quantitative RT-PCR was performed using the LightCycler (Roche Diagnostics Canada, QC, Canada). For a final reaction volume of 20 μL, the following reagents were added: 10 μL SYBR® Green Taq ReadyMix (Sigma-Aldrich, ON, Canada), 1.6 μL 25 mmol/L $MgCl_2$, 1 μL of each forward and reverse primers (Table 1), 5.4 μL H_2O, and 1 μL cDNA. Melting curve analysis was used to determine melting temperature (T_m) of specific amplification products and primer dimers. For each gene, the specific T_m values were used for the signal acquisition step (2–3 °C below T_m). The data was normalized to 18S RNA or β-actin mRNA to account for differences in reverse-transcription efficiencies and amount of template in the reaction mixtures.

Table 1. Oligonucleotide sequences for RT-PCR

Gene	Sequence
ANP	5′ CTGCTAGACCACCTGGAGGA 3′
	5′ AAGCTGTTGCAGCCTAGTCC 3′
BNP	5′ GACGGGCTGAGGTTGTTTTA 3′
	5′ ACTGTGGCAAGTTTGTGCTG 3′
MEF2A	5′ CAAATGGAGCTGGAAATGGT 3′
	5′ TCCGACTGTTCATTCCAACA 3′
MEF2C	5′ TACAACGAGCCGCATGAGAG 3′
	5′ CCTGTGTTACCTGCACTTGG 3′
IGF1R	5′ GGATGCGGTGTCCAATAACT 3′
	5′ TGGCAGCACTCATTGTTCTC 3′
SGK1	5′ TCTCTGGAAGCTTAGCAATC 3′
	5′ GCTTTGGAGCTAACACAATC 3′
18S rRNA	5′ GTAACCCGTTGAACCCCATT 3′
	5′ CCATCCAACGGTAGTAGCG 3′
ß-actin	5′ CATCGTACTCCTGCTTGCTG 3′
	5′ CCTCTATGCCAACACAGTGC 3′

Statistical analysis

All experimental data are expressed as means ± SD and were analysed by ANOVA and post-hoc analysis or by *t*-test as appropriate. A p value of 0.05 or less was considered significant.

Results

Diabetes-induced cardiac hypertrophy is associated with alteration of microRNAs

STZ-diabetic animals showed hyperglycemia (Diabetics: 22.0 ± 4.3 mmol/L; Controls: 7.2 ± 0.8 mmol/L; $p < 0.001$), reduced body weight gain (Diabetics: 26.9 ± 2.6 g; Controls: 19.6 ± 2.8 g; $p < 0.01$) and glucosuria (data not shown) at 2 months, compared to control animals. Our first aim was to establish whether diabetes causes characteristic cardiac changes in this model system. Hence, we carried out haemodynamic analysis to determine that diabetes induced functional alterations characteristic of diabetic cardiomyopathy. Basal heart rate was similar to these two groups. Diabetic animals showed decreased stroke volume, stroke work, ejection fraction and cardiac output. Furthermore, reduced d*P*/d*t* max and d*P*/d*t* min were evident in the diabetic animals. These findings indicate systolic and diastolic dysfunction and development of heart failure (Table 2). RT-PCR analysis of the heart tissues also showed increased expression of hypertrophic genes, ANP and BNP (Figure 1a and b).

We next performed RT-PCR analysis of other genes associated with hypertrophic changes. Our results show that heart tissues of the diabetic animals exhibit increased mRNA expression of MEF2A and MEF2C, two transcription factors associated myocardial hypertrophy (Figure 1c and d).

Our next objective was to determine whether diabetes leads to alteration of miRNAs in the heart. miRNA array analysis demonstrated alteration of a large number of miRNAs (Figure 2 and Figure S1, Supporting Information). Overall, 14 miRNAs showed statistically significant upregulation and 28 miRNA showed statistically significant downregulation (Figure 2).

Table 2. Haemodynamic assessment of mice

Parameters	Controls	Diabetic
Stroke volume (μL)	16.2 ± 0.4	7.9 ± 1.2**
Ejection fraction (%)	66.3 ± 3.4	31.5 ± 8.0**
Cardiac output (μL/min)	6757.0 ± 273.0	2740.7 ± 407.0**
Stroke work (mmHg* μL)	1522.0 ± 123.0	462.0 ± 156.0**
LV + d*P*/d*t* max (mmHg/s)	7996.0 ± 551.0	6137.0 ± 445.0*
LV − d*P*/d*t* min (mmHg/s)	−8136.0 ± 790.0	−5774.0 ± 449.0*

Data are expressed as means ± SE.
$n = 6$ in each group.
*$p < 0.05$ versus controls.
**$p < 0.01$ versus controls.

DOI: 10.1002/dmrr

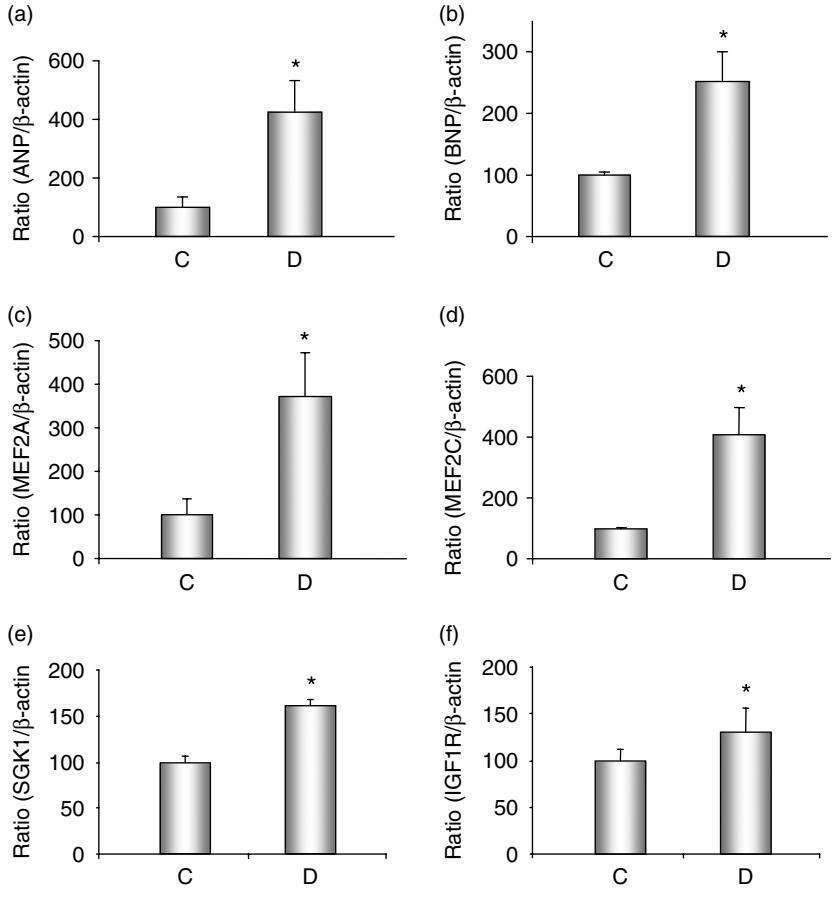

Figure 1. STZ-induced diabetic rats after 2 months of diabetes showed upregulation of ANP (a), BNP (b), MEF2A (c) and MEF2C (d), SGK1 (e) and IGF1R (f) mRNA. [mRNA are expressed as ratio of target to ß-actin, normalized to controls (C) and were compared to the diabetic group (D), $n = 6$/group, * = $p < 0.05$ compared to control group]

miR133a is downregulated in diabetic cardiomyopathy

One of the miRNA which was identified to be downregulated on the array study was miR133a. Hence, in the next set of experiments we focused on miR133a as its alterations were previously demonstrated in the heart in diabetic rabbits and miR133a have been shown to be downregulated in non-diabetic cardiac hypertrophy [11,16]. As an initial step, we validated the array data by using RT-PCR. miR133a was found to be significantly downregulated in the cardiac tissues of diabetic mice (Figure 3).

miR133a mediates glucose-induced cardiomyocyte hypertrophy

To further gain an insight into the role of miR133a in diabetic cardiomyopathy, we utilized an *in vitro* approach. We and others have used neonatal cardiomyocytes to study hypertrophy in both diabetic and non-diabetic conditions [22–29]. Exposure of cardiomyocytes to glucose and transfection with miR mimic showed no cytotoxicity, as evidenced by no significant differences among various groups in cell viability analysis (data not shown). Culture of myocytes in high glucose conditions for 48 h increased cell size and mRNA levels of ANP and BNP (Figure 4). As hypothesized, HG after 48 h caused downregulation of miRNA133a expression in these cells (Figure 3). Glucose-induced cardiomyocyte hypertrophy further occurred in conjunction with increased mRNA and protein expression of MEF2A and MEF2C, regulators of miR133 (Figures 5 and 6). To further establish a cause–effect relationship, we transfected glucose exposed cells with custom-synthesized miR133a mimics. Such transfection prevented glucose-induced cardiomyocyte hypertrophy as well as upregulation of hypertrophy associated factors ANP and BNP.

miR133a mediates its effects through SGK1 and IGFR1

We further expanded these studies to identify a mechanisms by which miR133a may regulate cardiac hypertrophy. A search for miR133a targets showed that it has multiple potential targets including SGK1 and IGF1R (http://www.microrna.org, http://www.targetscan.org). We and others have shown that both IGF1R and SGK1 are of importance in several chronic diabetic complications, including cardiomyocyte hypertrophy [30–33].

DOI: 10.1002/dmrr

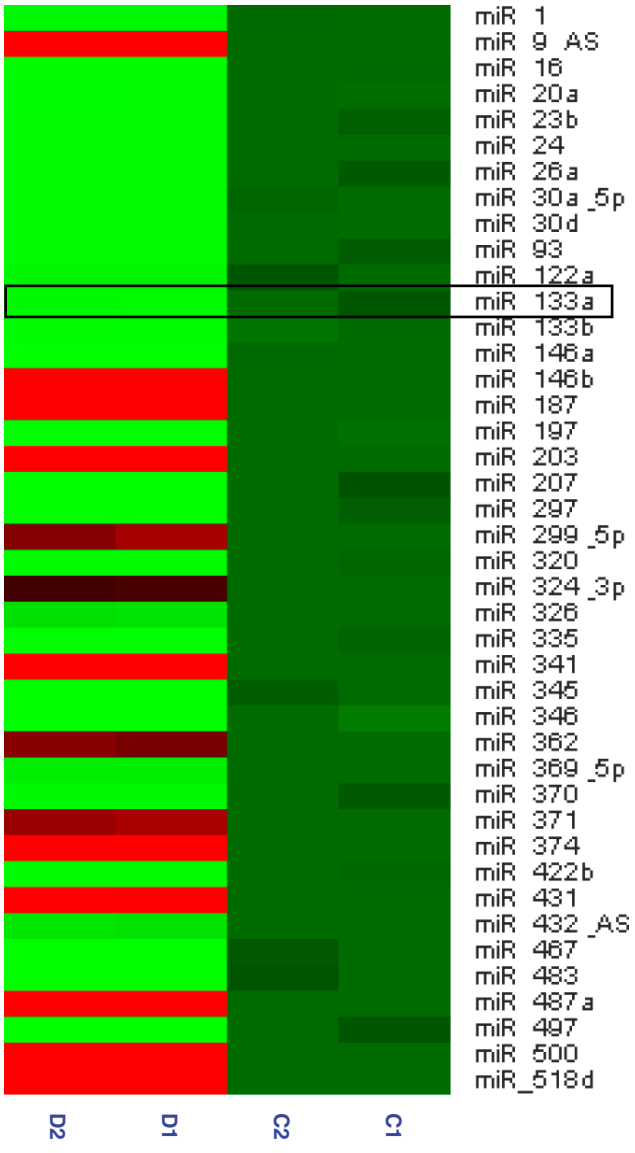

Figure 2. Representative miRNA expression profiles of selected miRNA which showed statistically significant alteration in the diabetic mice heart compared to controls. Hearts from mice were removed from control (C1, C2) and STZ-induced diabetic mice (D1, D2) after 2 months of diabetes when functional changes characteristic of diabetic cardiomyopathy were established. miRNAs were extracted by using mirVana miRNA isolation kit. Array analysis was performed using mirVana miRNA Bioarrays. [Red colour in diabetics (D1, D2) indicates significant upregulation; light green colour in diabetics (D1, D2) indicates significant downregulation (compared to dark green colour in controls C1, C2). BOX indicates miR133a; Figure S1 (Supporting Information) shows the expression of all miRNAs]. This figure is available in colour online at www.interscience.wiley.com/journal/dmrr

Hence, to investigate whether mi133a mediates its hypertrophic effects through IGF1R and SGK1, we investigated these two transcripts in the heart in diabetes and in the cardiomyocytes exposed to high glucose. Our results show that diabetes in the heart and high glucose in culture causes significant upregulation of these two transcripts (Figure 1e and f and Figures 5 and 6) in association with morphometrically demonstrable cardiomyocyte hypertrophy and ANP and BNP upregulation (Figure 4). Protein levels also showed similar upregulation (Figure 6). miR133a mimic transfection prevented glucose-induced upregulation of SGK1 and IGF1R mRNAs. As mentioned earlier, such transfection further prevented glucose-induced cardiomyocyte hypertrophy and caused diminution of glucose-induced ANP, BNP, MEF2A and MEF2C mRNA upregulation. No effects were seen with control transfection.

Discussion

We show for the first time that miR133a plays a key role in cardiomyocyte hypertrophy in diabetes. miR133a levels were decreased following 2 month of diabetes in the animal model. High levels of glucose produced a similar downregulation in cultured myocytes. Using custom miRNA mimics, we also show that miR133a regulates cardiomyocyte size and the expression of key genes involved in cellular hypertrophy. Finally, we provide a possible mechanistic pathway that suggests a role of SGK1 and IGF1R. Several interactive mechanisms, secondary to diabetic dysmetabolism are mechanistically involved in the pathogenesis of cardiomyopathy. At the nuclear level, we have previously demonstrated that p300, a HAT, plays an important role in diabetes-induced cardiomyocyte hypertrophy [22]. HDACs balance the action of p300 by promoting deacetylation. Recently, it was reported that the actions of HDACs are regulated by several miRNAs and vice versa [3,34,35]. It has been further postulated that miRNAs may be responsible for the paradoxical effect of the repression of cardiac hypertrophy by chemical inhibitors of HDACs [36]. Hence, it is plausible that key structural and functional deficits in diabetic cardiomyopathy are mediated by miRNAs. However, no studies have yet specifically examined miRNAs in the context of cardiomyocyte hypertrophy in diabetes. Hence, the purpose of this study was to investigate the role of miRNAs in such pathologic changes in the cardiomyocytes. We carried out miRNA array analysis in an animal model of chronic diabetes after first establishing that this model exhibits key functional features of diabetic cardiomyopathy. In these experiments, we identified alteration of several miRNAs. In total, 14 miRNAs were upregulated and 28 miRNAs were downregulated. As miRNAs play a fundamental role in gene expression, alteration of a large number in a chronic disease process is possible. One interesting miRNA that showed alteration was miR133a. miR133a has previously been shown to play an important role in muscle cell differentiation and proliferation [5]. Although, there is discrepancy as to specific miRNA alteration in non-diabetic cardiomyocyte hypertrophy (largely due various approaches and arrays used in these studies), some studies have shown downregulation of miR1 and miR133a in non-diabetic cardiac hypertrophy [5,16]. Recently, one study examined hearts from diabetic rabbits and reported

DOI: 10.1002/dmrr

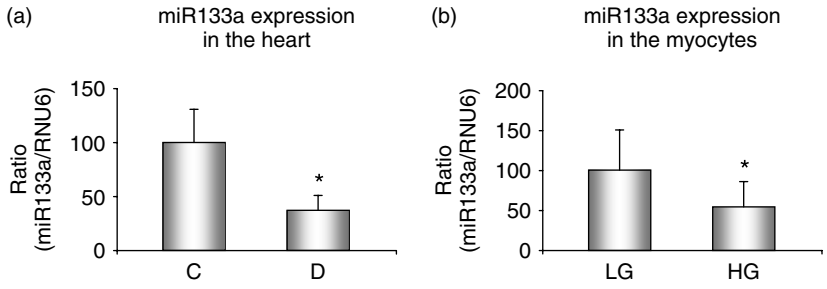

Figure 3. (a) Real-time RT-PCR analysis showing reduced miR-133a expression in the heart of diabetic (D) mice compared to controls (C). (b) Similar analyses in rat myocytes exposed to 25 mmol/L (HG) showed reduced miR133a expression compared to 5 mmol/L (LG) glucose. [miR133a quantities are expressed as ratio of target to RNU6B, normalized to C or LG. *$p < 0.05$ compared to the other group. Data are expressed as mean ± SD, $n = 6$/group]

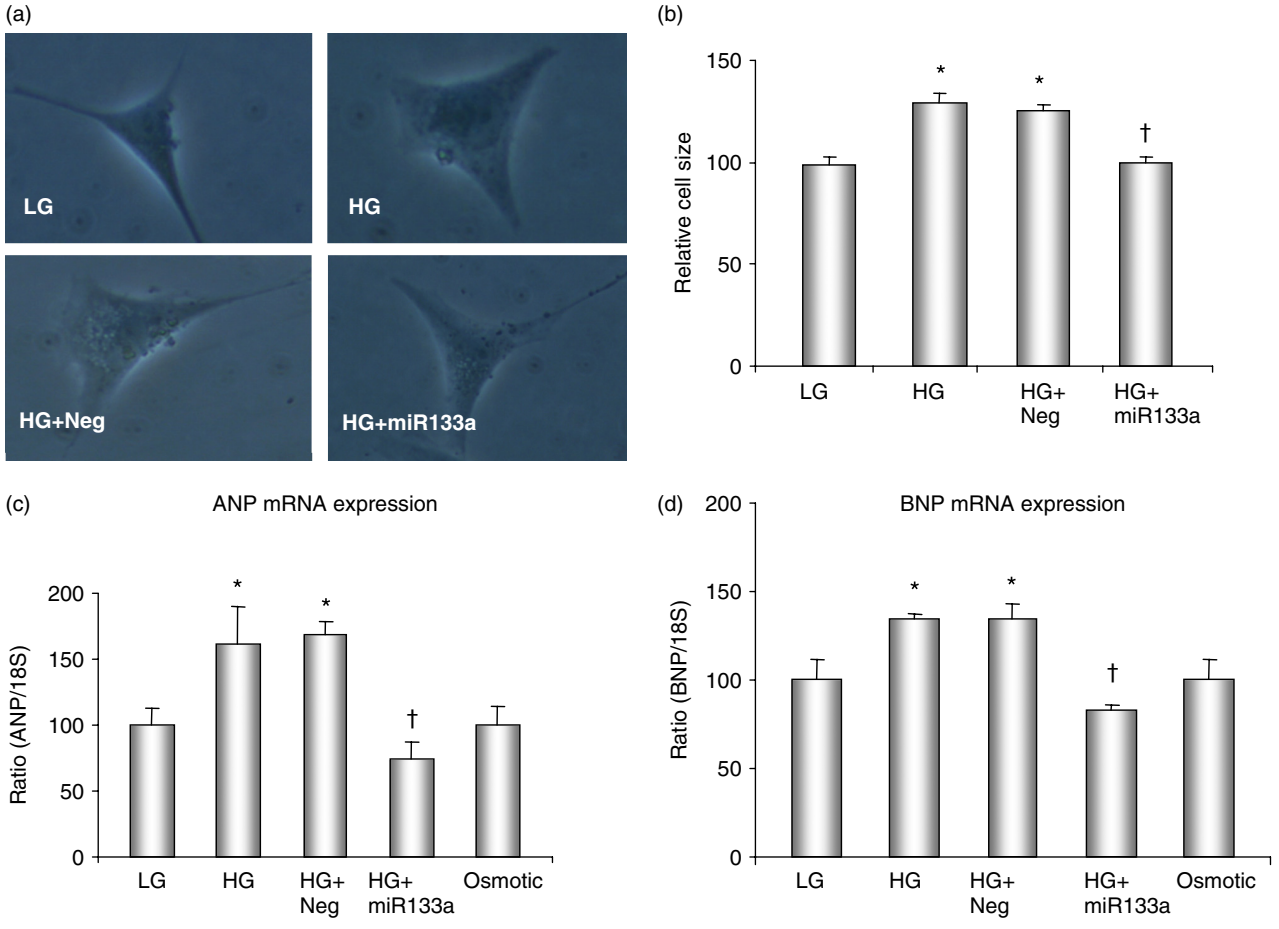

Figure 4. Representative photomicrographs (a) and morphometric analysis of neonatal rat cardiomyocytes (b), demonstrating cardiomyocyte hypertrophy in 25 mmol/L glucose (HG) compared to 5 mmol/L glucose (LG). In parallel, mRNA expression of ANP, BNP (c, d) were upregulated in HG. miR133a mimic transfection (HG + miR133a) prevented HG induced cardiomyocyte hypertrophy (a, b) and upregulation of mRNA expression of ANP, BNP (c, d). [mRNA data are expressed as ratio of target to 18S, normalized to LG. Data are expressed as mean ± SD, $n = 6$/group. * = $p < 0.05$ or less compared to LG, $^{\dagger}p < 0.05$ compared to HG. Neg = control miRNA, osmotic = 25 mmol/L L-glucose]. This figure is available in colour online at www.interscience.wiley.com/journal/dmrr

that increased miR133 may modulate HERG K+ channels causing QT prolongation [11].

Cardiomyocyte hypertrophy is an adaptive phenomenon to stress. Eventually hypertrophy leads loss of function and death of cardiomyocytes. Hence, understanding the mechanisms of cardiomyocyte hypertrophy will potentially lead novel therapeutic approaches [37]. Our results also show an interesting involvement of SGK1 and IGF1R in miR133a-mediated hypertrophic effects. We and others have previously demonstrated important roles of both SGK1 and IGF1R in chronic diabetic complications [30–33]. In the present study, our results demonstrate that glucose-induced cardiomyocyte hypertrophy is associated with IGF1R and SGK1 upregulation and SGK1 activation. These findings are in keeping with previous demonstration of upregulation of IGF1R and SGK1 in

DOI: 10.1002/dmrr

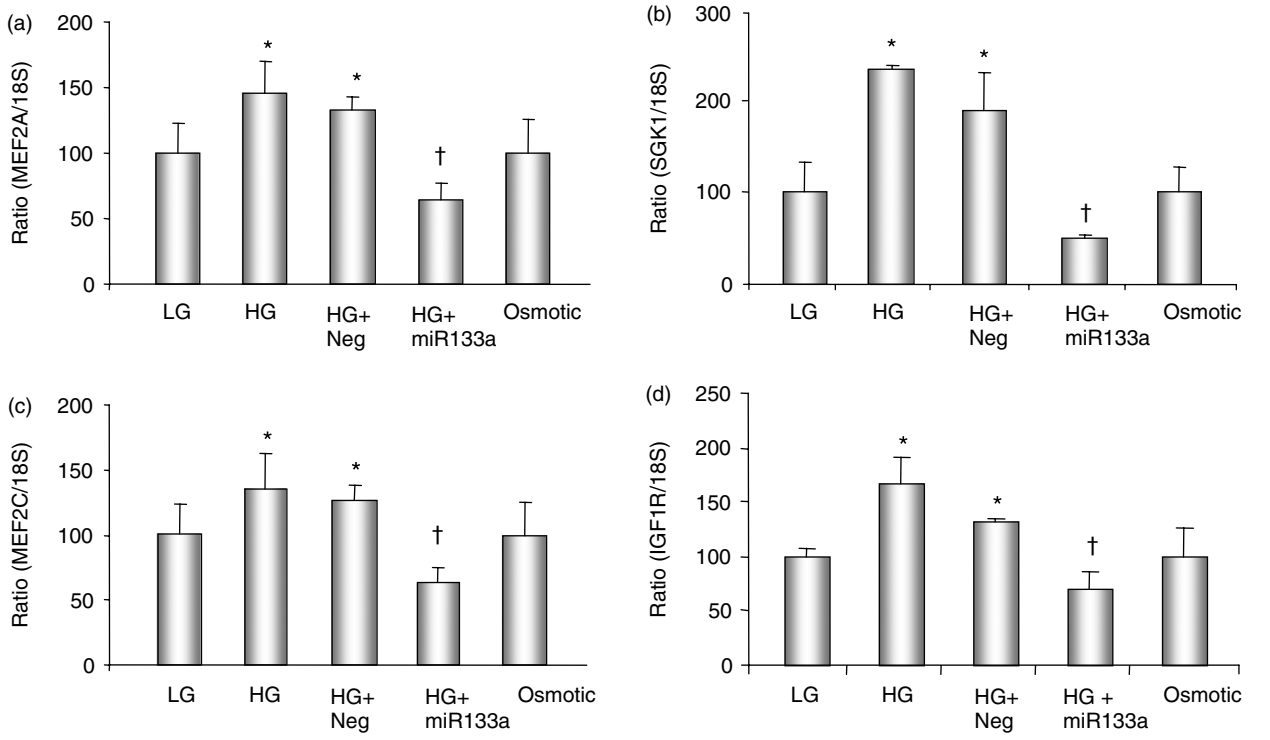

Figure 5. mRNA expression analysis in cardiomyocytes showed 25 mmol/L. Glucose (HG) induced mRNA upregulation of MEF2A (a), MEF2C (b), SGK1 (c), IGF1R (d) compared to 5 mmol/L glucose (LG). miR133a mimic transfection (HG + miR133a) prevented such upregulation. [mRNA data were expressed as a ratio of target to 18S (mean ± SD, $n = 6$/group), normalized to LG. * = $p < 0.05$, compared to LG, $^{\dagger}p < 0.05$ compared to HG, osmotic = 25 mmol/L L-glucose]

diabetic cardiomyopathy [30–33]. Both IGF1R and SGK1 mediate their effects through PKB activation. However, non-PKB dependent mechanisms may also be involved in SGK1 induced hypertrophy [30–33].

Another interesting finding of the present study was MEF2 transcription factor alteration associated with miR133a. We previously reported that glucose-induced cardiomyocyte hypertrophy is associated with increased activity of MEF2 [22]. Our present study adds to that finding and shows that MEF2A and MEF2C upregulation is prevented by miR133a mimics. Recently, it has been demonstrated that MEF2 may also regulate miR133a activity [10]. Therefore, it is possible that miR133a and MEF2 regulate each other in a positive feedback loop and culminate in cardiac dysfunction. Some investigators have however, demonstrated decreased MEF2 activity in diabetes [38]. It is to be noted that such studies were performed shortly after induction of diabetes by STZ. In the present study, we investigated hearts after 2 months of diabetes with evidence of cardiac failure. It is possible that, with longer duration, diabetes induces cardiac hypertrophy through MEF2 upregulation in a manner similar to non-diabetic cardiac hypertrophy [6,10,22]. It is further possible that miR133a may act through other targets. Of further interest in this context is that, based on target sequence analysis, endothelin converting enzyme mRNA has binding site for miR133a (http://www.microrna.org). We and others have demonstrated endothelin alteration in diabetic cardiomyopathy [20,23]. It is possible that such effects of endothelin may also be modulated by miRNAs. However, possible pathophysiologic roles of such additional miR133a targets need further evaluation. To further delineate roles of miR133a, treatment of diabetic animals using systemic miR133a mimics may be explored in future. Experiments are also needed to examine whether correction of hyperglycemia may prevent miR133a alteration and its downstream effects in diabetes.

In conclusion, we report a novel mechanism of glucose-induced cellular hypertrophy in diabetes. We show that diabetes leads to downregulation of miR133a and that in turn may regulate expression of key genes that are involved in cardiomyocyte hypertrophy. With better understanding of regulatory roles of miRNAs in diabetic cardiomyopathy and other disease processes, potential new avenues for RNA-based therapeutics may further be explored in future.

Supporting information

Supporting information may be found in the online version of this article.

Acknowledgements

These studies were supported by Heart and Stroke Foundation of Ontario.

DOI: 10.1002/dmrr

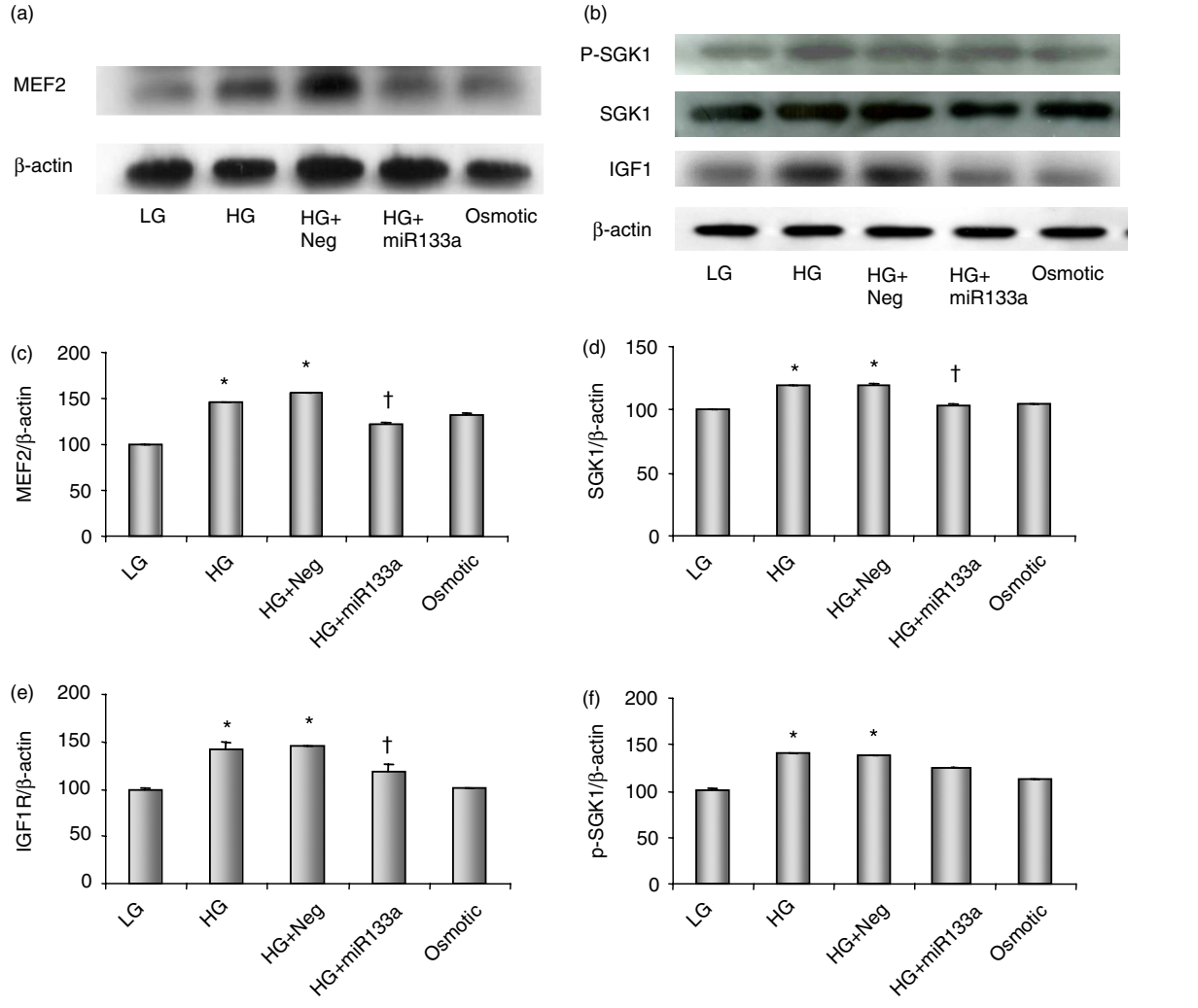

Figure 6. Representative western blots (a, b) showing that miR133a mimic transfection (HG + miR133a) prevented glucose-induced increased protein production of MEF2 (a) as well as total and phospho-SGK1 (P-SGK) and IGF1 R (b). "C–F" represent quantitative demonstrative analysis of the blots. [Quantitative data are expressed as a ratio to β-actin, normalized to LG, $n = 6$/group. $^{*}p < 0.05$ compared to LG, $^{\dagger}p < 0.05$ compared to HG, LG = 5 mmol/L glucose, HG = 25 mmol/L glucose, osmotic = 25 mmol/L L-glucose, neg = control miRNA]. This figure is available in colour online at www.interscience.wiley.com/journal/dmrr

References

1. Hayat SA, Patel B, Khattar RS, Malik RA. Diabetic cardiomyopathy: mechanisms, diagnosis and treatment. *Clin Sci (Lond)* 2004; **107**: 539–557.
2. Liu J. Control of protein synthesis and mRNA degradation by microRNAs. *Curr Opin Cell Biol* 2008; **20**: 214–221.
3. Chuang JC, Jones PA. Epigenetics and microRNAs. *Pediatr Res* 2007; **61**: 24R–29R.
4. Bartel DP. MicroRNAs: genomics, biogenesis, mechanism, and function. *Cell* 2004; **116**: 281–297.
5. Chen JF, Mandel EM, Thomson JM, *et al*. The role of microRNA-1 and microRNA-133 in skeletal muscle proliferation and differentiation. *Nat Genet* 2006; **38**: 228–233.
6. van Rooij E, Sutherland LB, Liu N, *et al*. A signature pattern of stress-responsive microRNAs that can evoke cardiac hypertrophy and heart failure. *Proc Natl Acad Sci USA* 2006; **103**: 18255–18260.
7. Cheng Y, Ji R, Yue J, *et al*. MicroRNAs are aberrantly expressed in hypertrophic heart: do they play a role in cardiac hypertrophy? *Am J Pathol* 2007; **170**: 1831–1840.
8. van Rooij E, Sutherland LB, Qi X, Richardson JA, Hill J, Olson EN. Control of stress-dependent cardiac growth and gene expression by a microRNA. *Science* 2007; **316**: 575–579.
9. Barringhaus KG, Zamore PD. MicroRNAs: regulating a change of heart. *Circulation* 2009; **119**: 2217–2224.
10. Liu N, Williams AH, Kim Y, *et al*. An intragenic MEF2-dependent enhancer directs muscle-specific expression of microRNAs 1 and 133. *Proc Natl Acad Sci USA* 2007; **104**: 20844–20849.
11. Xiao J, Luo X, Lin H, *et al*. MicroRNA miR-133 represses HERG K+ channel expression contributing to QT prolongation in diabetic hearts. *J Biol Chem* 2007; **282**: 12363–12367.
12. McCarthy JJ, Esser KA. MicroRNA-1 and microRNA-133a expression are decreased during skeletal muscle hypertrophy. *J Appl Physiol* 2007; **102**: 306–313.
13. Liu N, Bezprozvannaya S, Williams AH, *et al*. microRNA-133a regulates cardiomyocyte proliferation and suppresses smooth muscle gene expression in the heart. *Genes Dev* 2008; **22**: 3242–3254.
14. Ikeda S, Kong SW, Lu J, *et al*. Altered microRNA expression in human heart disease. *Physiol Genomics* 2007; **31**: 367–373.
15. Sayed D, Hong C, Chen IY, Lypowy J, Abdellatif M. MicroRNAs play an essential role in the development of cardiac hypertrophy. *Circ Res* 2007; **100**: 416–424.
16. Care A, Catalucci D, Felicetti F, *et al*. MicroRNA-133 controls cardiac hypertrophy. *Nat Med* 2007; **13**: 613–618.
17. Chen S, Evans T, Mukherjee K, Karmazyn M, Chakrabarti S. Diabetes-induced myocardial structural changes: role of endothelin-1 and its receptors. *J Mol Cell Cardiol* 2000; **32**: 1621–1629.

18. Evans T, Deng DX, Chen S, Chakrabarti S. Endothelin receptor blockade prevents augmented extracellular matrix component mRNA expression and capillary basement membrane thickening in the retina of diabetic and galactose-fed rats. *Diabetes* 2000; **49**: 662–666.
19. Farhangkhoee H, Khan ZA, Mukherjee S, *et al*. Heme oxygenase in diabetes-induced oxidative stress in the heart. *J Mol Cell Cardiol* 2003; **35**: 1439–1448.
20. Hileeto D, Cukiernik M, Mukherjee S, *et al*. Contributions of endothelin-1 and sodium hydrogen exchanger-1 in the diabetic myocardium. *Diabetes Metab Res Rev* 2002; **18**: 386–394.
21. Peng T, Zhang T, Lu X, Feng Q. JNK1/c-fos inhibits cardiomyocyte TNF-alpha expression via a negative crosstalk with ERK and p38 MAPK in endotoxemia. *Cardiovasc Res* 2009; **81**: 733–741.
22. Feng B, Chen S, Chiu J, George B, Chakrabarti S. Regulation of cardiomyocyte hypertrophy in diabetes at the transcriptional level. *Am J Physiol Endocrinol Metab* 2008; **294**: E1119–E1126.
23. Chen S, Khan ZA, Karmazyn M, Chakrabarti S. Role of endothelin-1, sodium hydrogen exchanger-1 and mitogen activated protein kinase (MAPK) activation in glucose-induced cardiomyocyte hypertrophy. *Diabetes Metab Res Rev* 2007; **23**: 356–367.
24. Chen S, Khan ZA, Barbin Y, Chakrabarti S. Pro-oxidant role of heme oxygenase in mediating glucose-induced endothelial cell damage. *Free Radic Res* 2004; **38**: 1301–1310.
25. Tu X, Miao L, Kang Y, *et al*. Effects of dl-praeruptorin A on cultured neonatal rat ventricular cardiomyocytes with hypertrophy induced by endothelin-1. *Methods Find Exp Clin Pharmacol* 2009; **31**: 231–236.
26. Chiu J, Xu BY, Chen S, Feng B, Chakrabarti S. Oxidative stress-induced, poly(ADP-ribose) polymerase-dependent upregulation of ET-1 expression in chronic diabetic complications. *Can J Physiol Pharmacol* 2008; **86**: 365–372.
27. Zeidan A, Javadov S, Chakrabarti S, Karmazyn M. Leptin-induced cardiomyocyte hypertrophy involves selective caveolae and RhoA/ROCK-dependent p38 MAPK translocation to nuclei. *Cardiovasc Res* 2008; **77**: 64–72.
28. Karmazyn M, Purdham DM, Rajapurohitam V, Zeidan A. Leptin as a cardiac hypertrophic factor: a potential target for therapeutics. *Trends Cardiovasc Med* 2007; **17**: 206–211.
29. Zeidan A, Javadov S, Karmazyn M. Essential role of Rho/ROCK-dependent processes and actin dynamics in mediating leptin-induced hypertrophy in rat neonatal ventricular myocytes. *Cardiovasc Res* 2006; **72**: 101–111.
30. Khan ZA, Barbin YP, Farhangkhoee H, Beier N, Scholz W, Chakrabarti S. Glucose-induced serum- and glucocorticoid-regulated kinase activation in oncofetal fibronectin expression. *Biochem Biophys Res Commun* 2005; **329**: 275–280.
31. Kuang HY, Zou W, Zhang GB, Gao XY, Yin HQ. The relationship of blood glucose and the expression of insulin-like growth factor-1 receptor mRNA in diabetic cardiomyopathy: a preliminary study with rats *Zhonghua Yi Xue Za Zhi*. 2007; **87**: 1249–1251.
32. Aoyama T, Matsui T, Novikov M, Park J, Hemmings B, Rosenzweig A. Serum and glucocorticoid-responsive kinase-1 regulates cardiomyocyte survival and hypertrophic response *Circulation* 2005; **111**: 1652–1659.
33. Saad S, Stevens VA, Wassef L, *et al*. High glucose transactivates the EGF receptor and up-regulates serum glucocorticoid kinase in the proximal tubule. *Kidney Int* 2005; **68**: 985–997.
34. Scott GK, Mattie MD, Berger CE, Benz SC, Benz CC. Rapid alteration of microRNA levels by histone deacetylase inhibition. *Cancer Res* 2006; **66**: 1277–1281.
35. Saito Y, Liang G, Egger G, *et al*. Specific activation of microRNA-127 with downregulation of the proto-oncogene BCL6 by chromatin-modifying drugs in human cancer cells. *Cancer Cell* 2006; **9**: 435–443.
36. van Rooij E, Liu N, Olson EN. MicroRNAs flex their muscles. *Trends Genet* 2008; **24**: 159–166.
37. Oka T, Komuro I. Molecular mechanisms underlying the transition of cardiac hypertrophy to heart failure. *Circ J* 2008; **72**(Suppl. A): A13–A16.
38. Mora S, Pessin JE. The MEF2A isoform is required for striated muscle-specific expression of the insulin-responsive GLUT4 glucose transporter. *J Biol Chem* 2000; **275**: 16323–16328.